

Crystal Structure of *Schizosaccharomyces pombe* Riboflavin Kinase Reveals a Novel ATP and Riboflavin-Binding Fold

Stefanie Bauer¹, Kristina Kemter², Adelbert Bacher², Robert Huber¹
Markus Fischer^{2*} and Stefan Steinbacher^{1*}

¹Max-Planck-Institut für Biochemie, Abteilung Strukturforschung, Am Klopferspitz 18a, D-82152 Martinsried, Germany

²Lehrstuhl für Organische Chemie und Biochemie Technische Universität München, Lichtenbergstr. 4 D-85747 Garching, Germany

The essential redox cofactors riboflavin monophosphate (FMN) and flavin adenine dinucleotide (FAD) are synthesised from their precursor, riboflavin, in sequential reactions by the metal-dependent riboflavin kinase and FAD synthetase. Here, we describe the 1.6 Å crystal structure of the *Schizosaccharomyces pombe* riboflavin kinase. The enzyme represents a novel family of phosphoryl transferring enzymes. It is a monomer comprising a central β -barrel clasped on one side by two C-terminal helices that display an L-like shape. The opposite side of the β -barrel serves as a platform for substrate binding as demonstrated by complexes with ADP and FMN. Formation of the ATP-binding site requires significant rearrangements in a short α -helix as compared to the substrate free form. The diphosphate moiety of ADP is covered by the glycine-rich flap I formed from parts of this α -helix. In contrast, no significant changes are observed upon binding of riboflavin. The ribityl side-chain might be covered by a rather flexible flap II. The unusual metal-binding site involves, in addition to the ADP phosphates, only the strictly conserved Thr45. This may explain the preference for zinc observed *in vitro*.

© 2003 Elsevier Science Ltd. All rights reserved

*Corresponding authors

Keywords: kinase; phosphoryl transferases; flavin cofactors; metal binding

Introduction

Kinases are of crucial importance in biology. Whereas protein kinases together with their counterplayers, the phosphatases, fulfil a central role in signal transduction and other regulatory processes, small molecule kinases are involved in diverse processes ranging from metabolic reactions over inactivation of antibiotics to cofactor biosynthesis. Kinases belong to the large group of nucleotide-binding proteins, which can be grouped into structurally related families.^{1,2} A recent survey of sequence and structure classification of kinases revealed that 98% of all sequences fall into only seven general structural folds for which three-dimensional structures are known.³

Flavoenzymes⁴ contain flavin nucleotides as redox cofactors, either riboflavin monophosphate (FMN) or flavin adenine dinucleotide (FAD). Both are synthesised from the precursor, riboflavin (vitamin B₂). Plants and many microorganisms are able to synthesise riboflavin, whereas animals and certain microorganisms depend on riboflavin uptake. All organisms are able to convert the precursor, riboflavin, into the active flavin nucleotide cofactors (Figure 1). The formation of FAD depends on the sequential utilisation of two molecules of ATP in reactions that first involve the phosphorylation of riboflavin to form FMN by riboflavin kinase and then the adenylation of the latter to form FAD, a reaction catalysed by FAD synthetase.

Flavokinases have been reported from a variety of species. In many prokaryotic organisms, riboflavin kinase and FAD synthetase activity are present in a single, bifunctional enzyme.^{5,6} In contrast, both enzymes could be purified separately in eukaryotic organisms⁷ including *Saccharomyces cerevisiae* (FMN1) and *S. pombe*. In addition the *ribR* gene product of *Bacillus subtilis* was shown to encode a monofunctional riboflavin kinase.^{8,9}

Present address: S. Steinbacher, Division of Chemistry and Chemical Engineering, California Institute of Technology, Mail Code 114-96, Pasadena, CA 91125, USA.

Abbreviations used: FAD, flavin adenine dinucleotide.

E-mail addresses of the corresponding authors: markus.fischer@ch.tum.de; steinbac@biochem.mpg.de; steinbac@caltech.edu

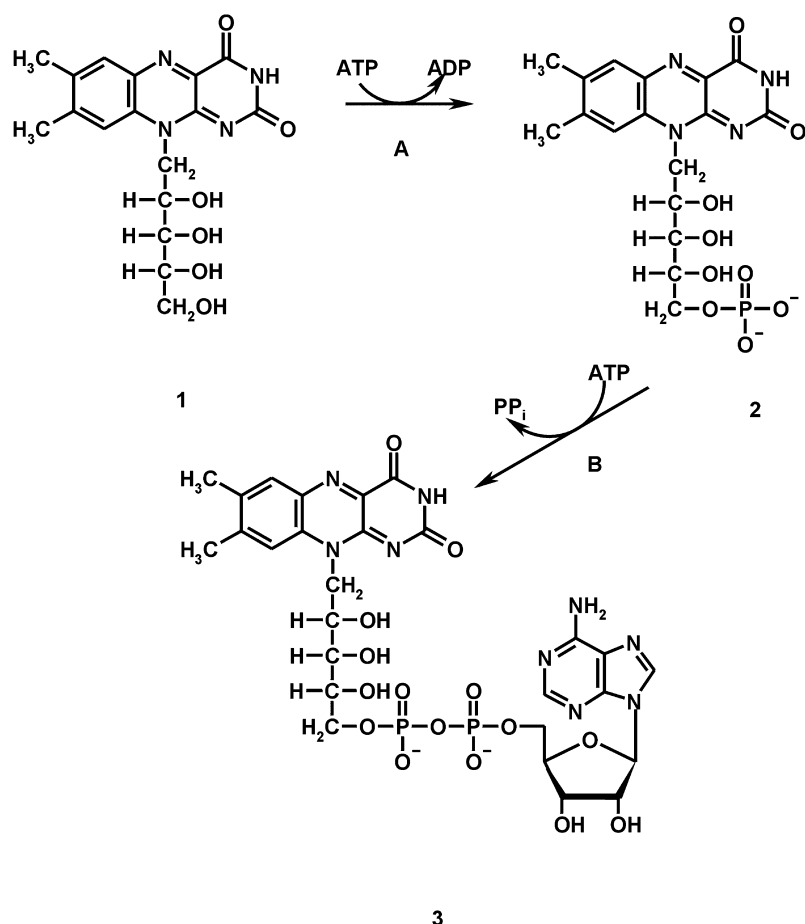


Figure 1. Reaction catalysed by riboflavin kinase and FAD synthetase. 1, Riboflavin; 2, FMN; 3, FAD.

Like all phosphoryl-transferring enzymes, riboflavin kinase requires divalent metal ions for activity. In contrast to most other ATP-dependent enzymes that prefer Mg^{2+} , riboflavin kinase from rat liver shows an activity increase by a factor of 1.8 with low concentrations of Zn^{2+} and an optimal activity at pH 9.3, indicating its unusual properties.¹⁰

As sequence comparison did not reveal homologues with known three-dimensional structure, riboflavin kinase is suggested to form a novel family of phosphoryl-transferring enzymes. Here, we describe the first crystal structure of a riboflavin kinase from *S. pombe* in its substrate free form and in complex with either the products ADP and FMN or with ADP and zinc.

Table 1. Statistics for data collection and phasing

	NativI	TM ^a	BP ^b	TaBr ^c	TM + BP	NativII	ADP	ADP + FMN	ADP + Zn
Space group	<i>P</i> ₆ ,22	<i>P</i> ₁	<i>P</i> ₁	<i>P</i> ₁					
Resolution range (Å)	20–2.9	20–3.0	20–3.8	20–3.5	20–3.0	20–2.1	20–2.0	20–2.45	20–1.6
Last shell (Å)	2.93–2.9	3.05–3.0	3.87–3.8	3.58–3.5	3.16–3.0	2.13–2.1	2.07–2.0	2.54–2.45	1.64–1.6
Independent reflections	4906	4435	2596	2294	4442	11,946	21,249	11,694	42,651
R_{merge}^d overall (%)	8.8	9.6	16.1	12.5	9.0	9.9	6.1	4.1	4.3
Outermost shell (%)	28.3	31.6	29.6	24.5	28.1	34.2	41.2	24.2	40.4
Completeness overall (%)	98.6	99.4	98.5	90.7	97.8	97.3	95.1	96.6	92.5
Outermost shell (%)	98.2	99.5	97.1	94.0	97.2	97.3	92.4	93.9	88.5
Multiplicity	6.6	5.0	3.4	6.1	6.8	8.8	3.2	2.2	3.0
R_{iso}		27.5	23.5	10.4	24.7				
R_{Cullis}		0.93	0.63	0.90	0.66				

^a Thiomersal.

^b 2,5-Bis-chloromercuri-4-nitrophenol.

^c Ta₆Br₁₄.

^d $R_{merge} = \sum_{hkl} [(\sum_i |I_i - \langle I \rangle|) / \sum_i I_i]$; $R_{iso} = \sum |F_{PH} - F_P| / \sum F_P$; $R_{Cullis} = \text{r.m.s. lack of closure} / \text{r.m.s. isomorphous differences}$; Phasing power $\langle |F_H| \rangle / \text{r.m.s. lack of closure}$.

Table 2. Refinement statistics

	NativII	ADP	ADP + FMN	ADP + Zn
Resolution range	20–2.1	20–2.0	20–2.45	20–1.60
Reflections (working set)	11,269	20,211	11,079	40,509
Reflections (test set)	611	1038	602	2142
R_{cryst}^a (%)	22.0	23.8	22.7	21.9
R_{free}^a (%)	26.6	27.3	28.3	25.2
Non-hydrogen protein atoms	1149	2533	2533	2533
Solvent molecules	129	154	192	270
Ligand atoms		53	115	55
<i>Rmsd</i>				
Bond length (Å)	0.01	0.007	0.010	0.008
Bond angle (deg.)	1.3	1.7	1.3	1.3

$$^a R_{\text{cryst}} = \frac{\sum_{hkl} |F_{\text{obs}}| - k |F_{\text{calc}}|}{\sum_{hkl} |F_{\text{obs}}|}; \quad R_{\text{free}} = \frac{\sum_{hkl} |F_{\text{obs}}| - k |F_{\text{calc}}|}{\sum_{hkl} |F_{\text{obs}}|}$$

Results and Discussion

Structure determination

Riboflavin kinase of *S. pombe* was expressed in a recombinant *Escherichia coli* strain as a functional protein. The crystal structure of the riboflavin kinase from *S. pombe* was solved by multiple isomorphous replacement in the absence of ligands (Table 1). The model was refined at 2.1 Å to an R -factor of 22.0% and an R_{free} of 27.0% (Table 2). The crystals belonged to the space group $P6_122$ with one monomer in the asymmetric unit, which reflects the solution state of the enzyme. The final model contains 142 residues out of 163. No electron density is present for residues 1–9 and 82–93.

Soaking these crystals with 10 mM solutions of ATP, ADP or FMN did not result in the observation of any additional electron density, hence suggesting that the binding sites are blocked by crystal contacts. Co-crystallisation of the enzyme with ADP afforded a new triclinic crystal form with two molecules in the asymmetric unit that clearly displayed the bound ADP. In that crystal form, the riboflavin-binding site was accessible in both molecules in the asymmetric unit, and soaking with the product, FMN, was conducive to a clear electron density for the isoalloxazine ring of FMN. The zinc ion could be unambiguously defined in ADP co-crystals soaked with 5 mM Zn^{2+} . The structures of the ADP-containing complexes were solved by molecular replacement and refined at a resolution of 2.0 Å (ADP), 2.45 Å (ADP + FMN) and 1.6 Å (ADP + Zn). The final models of the three complexes consist of 154 amino acid residues with an R factor of 23.8% (ADP), 22.5% (ADP + FMN) and 22% (ADP + Zn) and an R_{free} of 27.3% (ADP), 28.1% (ADP + FMN) and 25.2% (ADP + Zn). Table 2 gives a summary of the refinement statistics.

Overall three-dimensional architecture

Riboflavin kinase of *S. pombe* consists of a single domain of rather globular shape with a diameter of about 36 Å (Figure 2(a)). As a prominent feature, the N-terminal part of helix H3 protrudes adjacent to the substrate-binding platform where it contributes to the riboflavin-binding site. The crystallographic model of *S. pombe* riboflavin kinase comprises residues 10 to 82 and 94 to 162, which fold into six β -strands, four α -helices and the connecting loops. The six β -strands are highly twisted to form a flattened β -barrel comprising two antiparallel β -sheets lying on top of each other. Figure 3 shows the secondary structure elements of the *S. pombe* riboflavin kinase. The upper β -sheet that provides the substrate-binding platform is composed of five β -strands of topology 1-2-5-4-3. The lower β -sheet is composed of four β -strands of topology 1-6-3-4. The β -strands S1, S3 and S4 are shared between both β -sheets. On the upper β -sheet, a short α -helix H1 (residues 36–41), which is essential for ATP binding, is inserted between strands S1 and S2. Between strands S4 and S5 (from Gly82 to Ser94), there is no electron density for 11 residues, so these are likely very flexible. Another short helix H2 is inserted between β -strands S2 and S3 (residues 53–60). The C-terminal helical segment consists of a longer α -helix (residues 129–147) and a short 3_{10} -helix (residues 150–158) perpendicular to the former, which display an L-like shape and clasp the central β -barrel.

In the ADP-cocrystals the loop between β -strands S4 and S5 (residues 83–93) becomes ordered mainly due to crystal contacts. As this otherwise flexible region is adjacent to the FMN-binding site, it might be involved in catalysis by forming a flexible flap that covers FMN. Therefore, we designate this loop flap II (see below).

Active site architecture

Attempts to identify the substrate-binding sites in the hexagonal crystals obtained for the substrate free enzyme by soaking failed. However, co-crystallisation with 2 mM ADP afforded a new triclinic crystal form with two molecules in the asymmetric unit (Figure 2(b)). In these crystals, clear electron density for the ADP molecule was visible in the vicinity of helix H1 (Figure 4(a)). Soaking of these crystals with the second reaction product FMN in the presence of ADP yielded bright yellow crystals that showed the electron density for the isoalloxazine ring in a cleft formed by the N-terminal half of α -helix H3 and the loop between β -strand S6 and α -helix H3 (Figure 4(b)). The phosphoribityl side-chain is rather disordered but appears to assume an extended conformation that is conducive to a close contact between the β phosphate of ADP and the phosphate group of the phosphoribityl chain in direct neighbourhood to the strictly conserved residue Asn47. The nearby

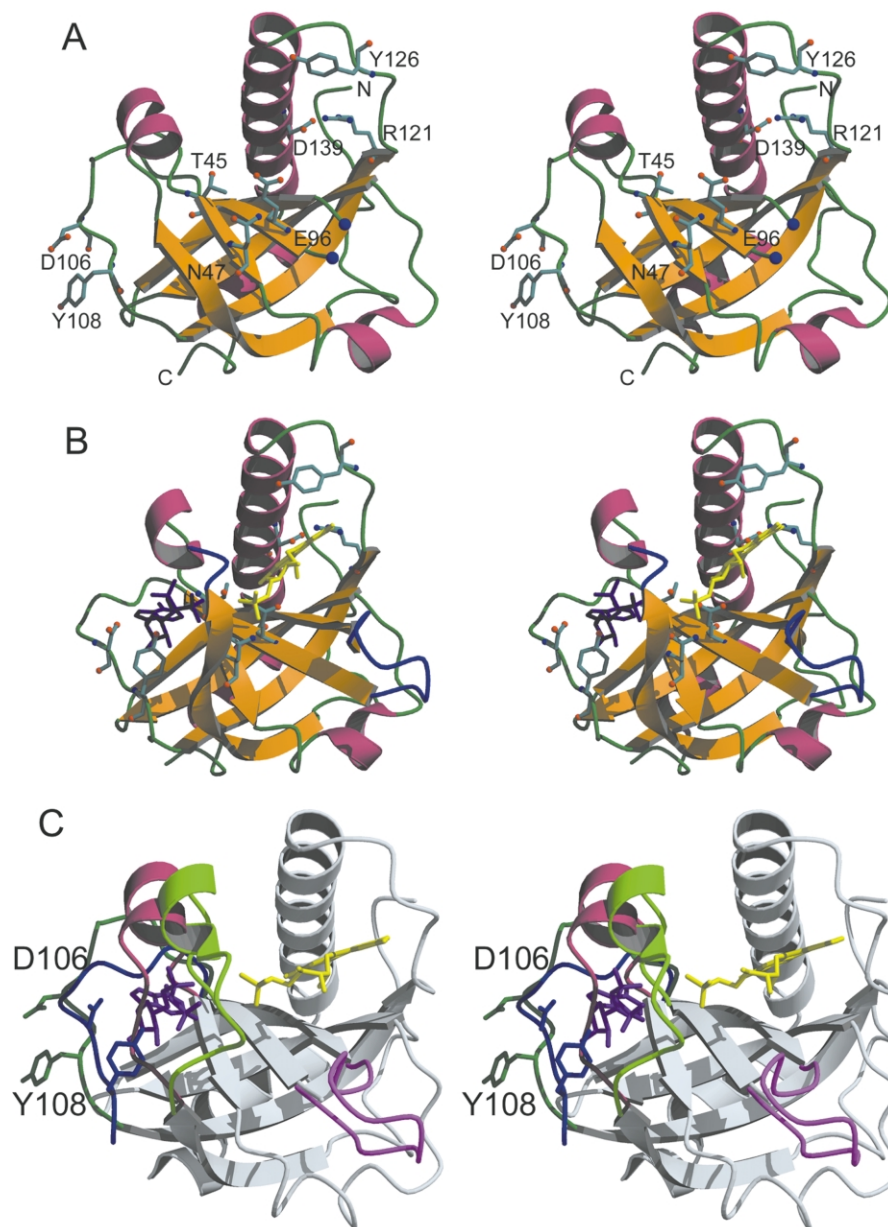


Figure 2. Stereo drawings of the *S. pombe* riboflavin kinase structure (a) without bound substrates and (b) co-crystallised with ADP and FMN introduced by soaking. Secondary structure elements are coloured: α -helix (red) and β -sheets (yellow). (c) Comparison of ligand free (red and dark green) and ADP-bound (light green and blue) conformations of riboflavin kinase. In the absence of nucleotides flap I collapses into the adenosine-binding site. Conserved residues that change their orientation upon ADP binding are shown as ball-and-stick models. Asp106 and Tyr108 help to position the ribose moiety. Flap II is depicted in pink.

Glu96 is able to form hydrogen bonds to O4 and O5 of the ribityl side-chain. This site of phosphoryl transfer is covered by the loop between β -strand S2 and α -helix H1 that includes residues Gly33 to Gly37, a region that we designate flap I. However, the electron density of the glycine-rich flap I is weak around Gly35 and for the side-chain of Arg36. The precise conformation might be influenced by nearby crystal contacts. In the hexagonal crystals the entire binding sites for ATP and riboflavin are completely blocked by crystal contacts, which explains why soaking experiments failed.

The phosphoribityl side-chain of FMN remains markedly exposed to the solvent in our structure, which is quite unusual as the necessity to shield the substrates from the solvent to prevent uncontrolled ATP-hydrolysis has been recognised as a general principle of phosphoryl-transferring enzymes.² This is generally achieved by large domain motions or by flexible loop structures similar to the glycine-rich loop of protein kinases. In riboflavin kinase the loop between β -strands S4 and S5 (Ser81 to Ser94), designated flap II, is a prime candidate to serve this purpose (Figure 2(a) and (b)). A functional role of flap II is supported

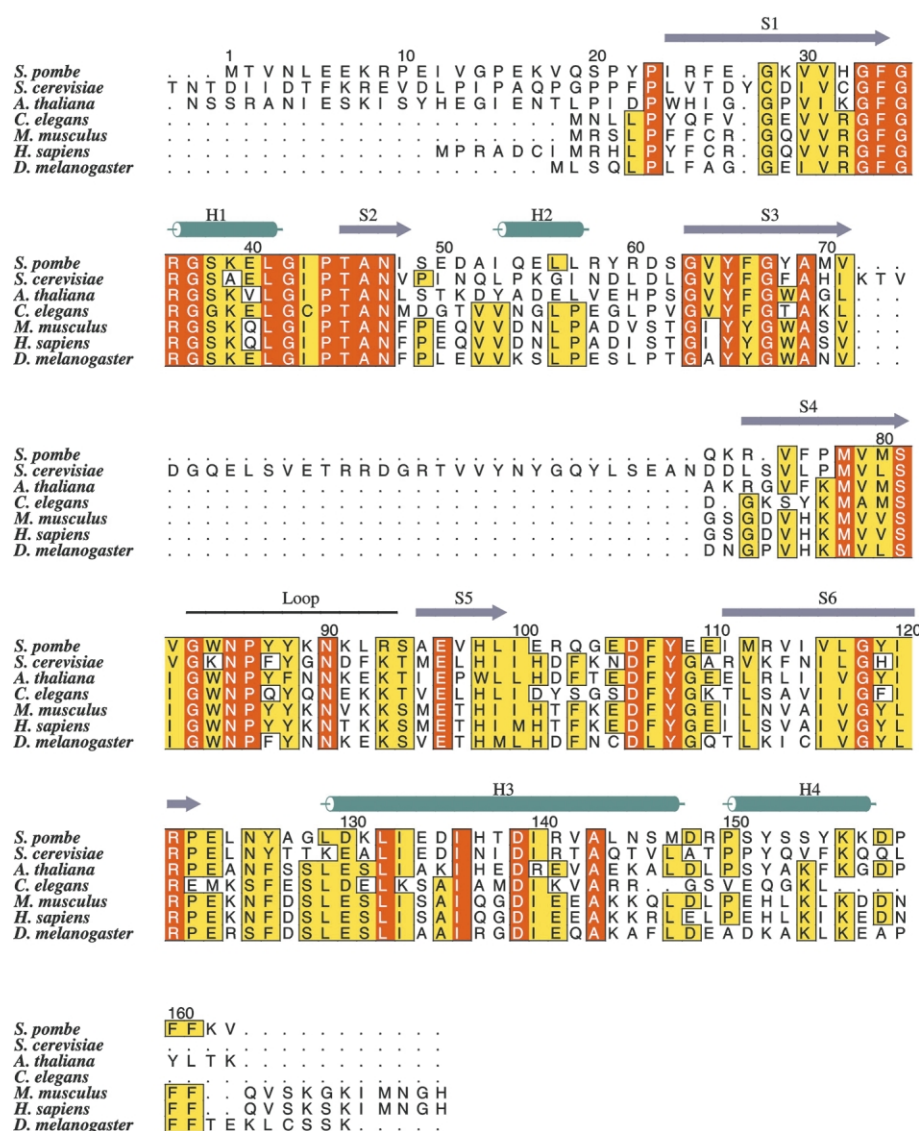


Figure 3. Secondary structure assignment of ligand free *S. pombe* riboflavin kinase and sequence alignment with homologous proteins. The sequence numbering corresponds to the *S. pombe* enzyme. Secondary structure elements (green, α -helices; blue, β -strands) found in *S. pombe* riboflavin kinase are shown above the sequences. Identical residues (red background) and conserved residues (yellow background) are indicated. The Figure was prepared with ALSRIPT.³⁶

by the presence of conserved residues with a consensus sequence Ser81-x-Gly-x-Asn-Pro-x-x-Asn90.

Comparison of the substrate free form and the liganded form of riboflavin kinase reveals significant structural flexibility around helix H1 and the loop connecting β -strands S5 and S6 that accompanies binding of ADP (Figure 2(c)). A number of glycine residues at the N and C-terminal boundaries of α -helix H3 crucially contribute the rearrangement of the ATP-binding site. The entire region spanning His32 to Asn47 notably represents a highly conserved part of the molecule that is involved in ATP-binding and the dynamic formation of the binding site. It contains the invariant sequence motif Gly42-x-ProThrAlaAsn where x represents a large hydrophobic residue.

The binding sites for ADP and FMN identified here correspond nicely to the distribution of conserved residues that scatter over the entire substrate-binding platform (Figure 2(a)). In addition to Asn47 and Glu96 at the site of phosphoryl transfer, conserved residues participate in the binding of riboflavin (Arg121 and Asp139), ATP (His98, Asp106 and Tyr108) or the divalent metal ion (Thr45).

Binding of ATP and riboflavin

The active site can be subdivided into two binding sites for ATP and riboflavin, respectively, which were characterised by bound products ADP and FMN in the absence of divalent cations. Figures 4 and 5 show the riboflavin and

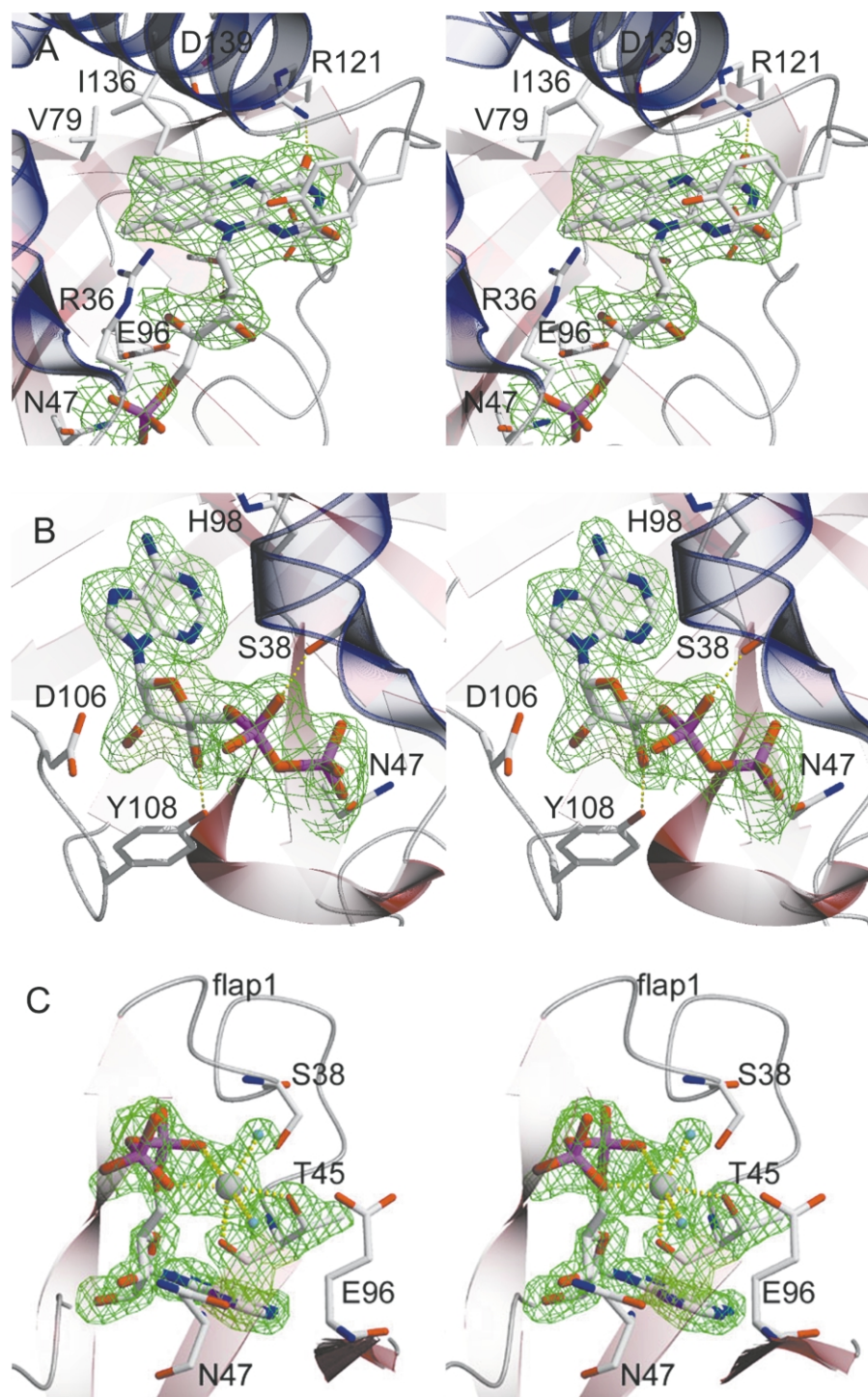


Figure 4. Electron densities for bound product molecules. (a) Stereo drawings of the riboflavin-binding site from *S. pombe* riboflavin kinase with bound FMN. (b) Stereo drawings of the ATP-binding site with bound ADP. Residues that show hydrophobic or hydrogen bond interactions are shown. The final omit $2F_{\text{obs}} - F_{\text{calc}}$ electron density maps covering the product molecules are contoured at 1 sigma. Residues that show hydrophobic or hydrogen bond interactions are shown. (c) Refined omit $2F_{\text{obs}} - F_{\text{calc}}$ electron density map at the zinc-binding site at 1.6 Å resolution.

ATP-binding sites of riboflavin kinase from *S. pombe* with the final $2F_{\text{obs}} - F_{\text{calc}}$ electron density map covering the bound molecules. The riboflavin-binding site (Figure 4(a)) is formed by the C-terminal α -helix H3 and the loop connecting α -helix H3 and β -strand S3. The isoalloxazine ring

of the FMN molecule is bound to a hydrophobic pocket that consists of Val79, Tyr126, Leu129, Leu132 and Ile136. Besides these residues, the invariant residues Arg121 and Asp139, which form a salt bridge, interact with the O4 carbonyl of FMN *via* the amidino group of Arg121. In detail,

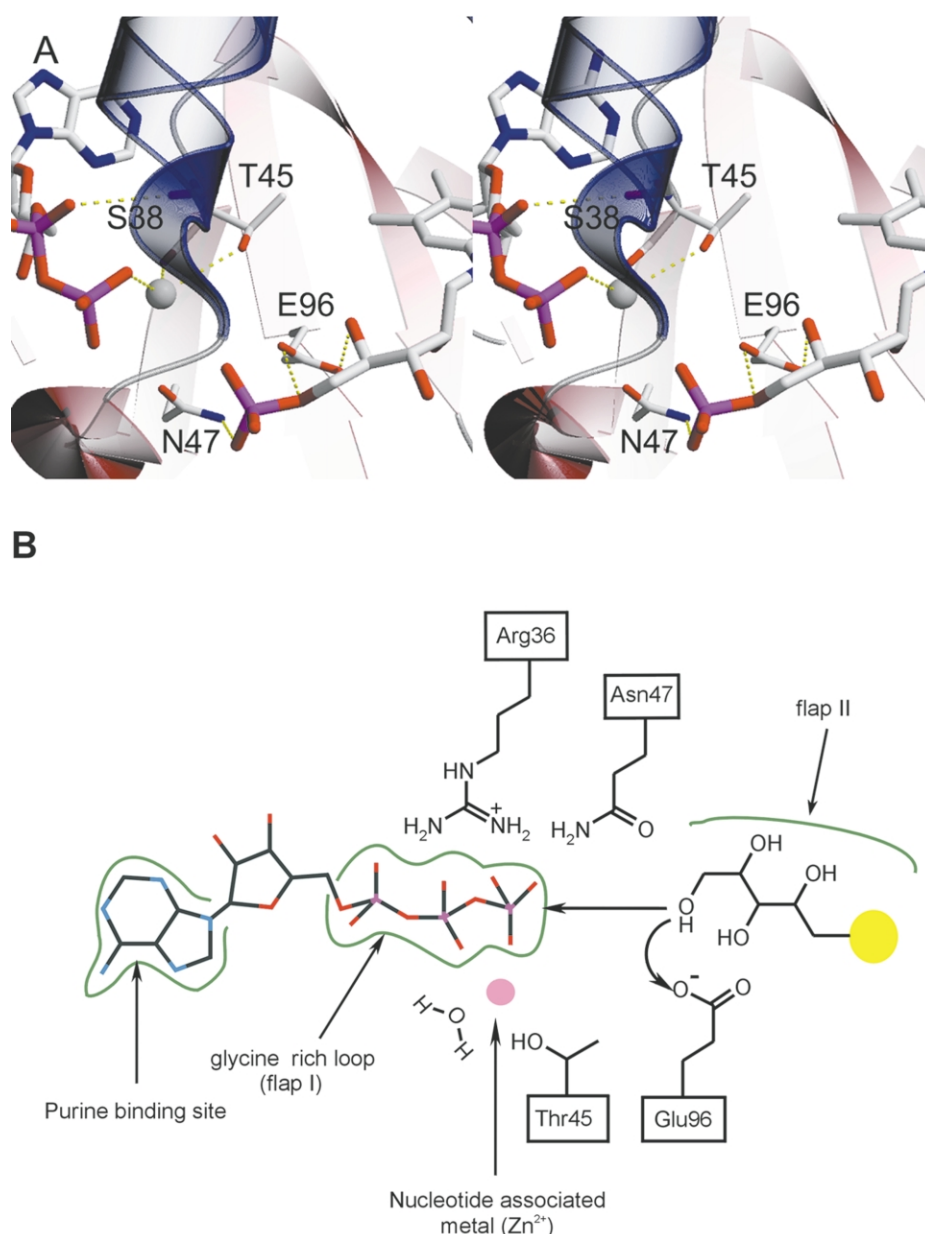


Figure 5. Proposed catalytic mechanism of riboflavin synthase. (a) Stereo drawings of the active site of the riboflavin kinase. Bound FMN and ADP are shown as ball-and-stick models. The position of the zinc ion was taken from ADP + Zn complex. Flap I covers the β and γ phosphate-binding sites. (b) Residues involved in catalysis.

several hydrogen bonds to polar groups of the FMN ring are formed that involve main-chain and side-chain interactions (Figure 6). The carbonyl oxygen O4 and the N3H of FMN hydrogen bond with the amide and carbonyl groups of Leu124, respectively. The guanidino group of the Arg121 side-chain and the carbonyl oxygen O4 of FMN form a hydrogen bond. The ribityl side-chain of bound FMN is largely disordered but in an extended conformation, which is necessary to span the distance to the ADP molecule, it can be stabilised by hydrogen bonds of the hydroxyl group of Ser81, with the hydroxyl group OH2 of the ribityl chain, and by interactions of the carboxylate group of Glu96 with OH4. In addition,

Glu96 is positioned in the vicinity of the 5'-phosphoryl moiety.

The ATP-binding site of riboflavin kinase (Figure 4(b)) is located in the vicinity of α -helix H1 and comprises the loops preceding and following this helix and the loop connecting β -strand S5 and S6. The binding of the adenosyl ring of the ADP molecule is enhanced by hydrogen bond interactions of the backbone and side-chains. The N1 and 6-amino group of the adenosyl ring hydrogen bond to the amide and carbonyl groups of Leu99, respectively. Interactions of the ribosyl ring are formed by a hydrogen bond between the amino group of the Lys39 side-chain and O4 and a van der Waals contact between the carboxyl oxygen of

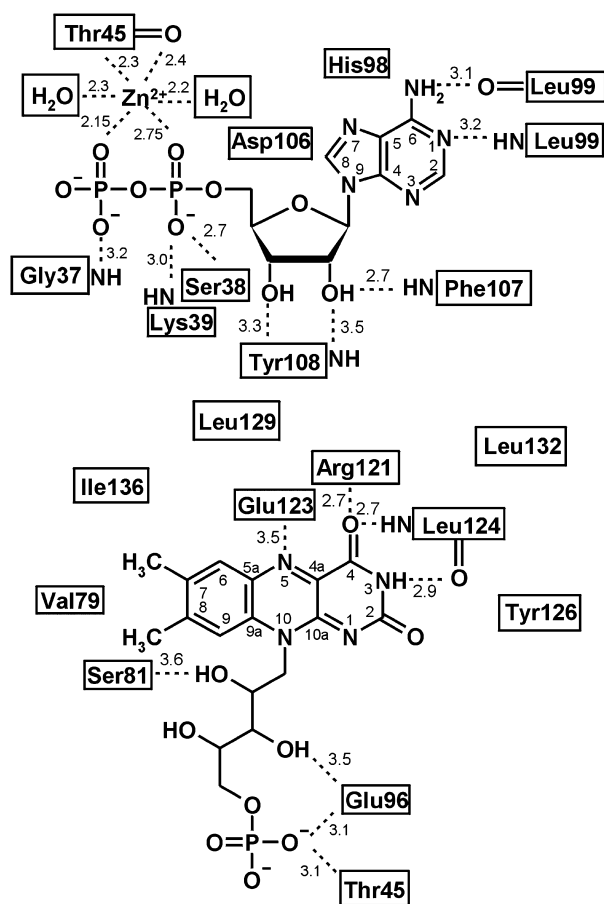


Figure 6. Schematic representation of product interactions.

Asp106 and O4. Hydrogen bond interactions of the hydroxyl groups of the ribosyl ring are formed by the amide group of Phe107 with 2'-OH, the amide group of Tyr108 with the 2'-OH and between the hydroxyl group of Tyr108 and 3'-OH. The diphosphoryl group of the ADP molecule is stabilised by hydrogen bond interactions of the amino group of Lys39 with one of the P α oxygen atoms. Sequence comparison indicates that most of the residues that contribute to the ADP and FMN binding by hydrogen bond or hydrophobic interactions are well conserved or conservatively replaced in all organisms.

Binding of the divalent metal ion

Phosphoryl-transferring enzymes have a number of principles in common that often include carboxylic acids as metal ligands and a general base that activates the substrate.² Riboflavin kinase is active in the presence of Mg²⁺ and other divalent metal ions but shows a higher activity with Zn²⁺. Only three invariant residues are found near the active site, namely Thr45, Asn47 and Glu96 that might function as ligands to the metal.

An ADP-containing co-crystal was soaked with Zn²⁺ and analysed at 1.6 Å resolution. This revealed a well defined metal-binding site

(Figure 4(c)). The zinc ion is co-ordinated by α and β phosphate oxygen atoms and the carbonyl and side-chain oxygen atoms of Thr45. The co-ordination sphere of Zn²⁺ is completed by two water molecules to yield a distorted octahedral geometry, which is also usually observed for Mg²⁺. Interestingly, the nearby Glu96 and Asn47 do not contribute to metal binding, which leaves these residues a role in coordination of the ribityl side-chain or the function of a general base during phosphoryl transfer. For the latter task Glu96 seems ideally suited. The side-chain of Asn47 is observed in two conformations but in none of them is it near enough to the zinc to serve as ligand. The second conformation of Asn47 is not so well defined so the description will be limited to the first conformation.

From geometric considerations it is likely that the water molecule distal to the carbonyl oxygen of Thr45 (closer to flap I) occupies the position of the γ phosphate oxygen in the metal-ATP complex. The shortest distance from the free β phosphate oxygen pointing towards the metal to this water molecule is 3.7 Å, whereas it is 5.1 Å to the equatorial water molecule. In that case, backbone amides of flap II ranging from Phe34 to Ser38 might contribute additional hydrogen bonds to the γ phosphate-binding site, which is complemented by the strictly conserved Asn47.

The metal-binding site involves both the side-chain hydroxyl and backbone carbonyl group oxygen of Thr45. This binding mode is rather unusual as in general only the side-chain hydroxyl group of Ser/Thr residues is observed as ligand to Mg²⁺ like in P-loop containing proteins as F₁-ATPase¹¹ or GTP-binding proteins.² There it forms a bidentate co-ordination with the β and γ phosphate groups of the nucleotide. There are no experimental data as to whether riboflavin kinase indeed uses Zn²⁺ *in vivo*. An increased activity by a factor of about 1.8 compared to Mg²⁺¹⁰ might be easily compensated by the higher availability of the latter. It is known that the total concentration of zinc, the zinc quota, in *E. coli* is about 0.2 mM and highly regulated by zinc homeostasis with an overcapacity of zinc sequestration.¹² The total cellular Mg²⁺ level, in contrast, has been reported to be in the range of 14 to 20 mM for most mammalian cells with about 0.25 to 1 mM as free Mg²⁺ and about 90% of ATP present as MgATP.¹³ In any case, riboflavin kinase might be a promiscuous enzyme *in vivo*.

Reaction mechanism

A commonly discussed mechanism of phosphoryl transfer involves an in-line attack of the nucleophile on the γ phosphate of ATP. This can be described either with an associative or dissociative transition state. The pentavalent transition state of the associative mechanism shows a net charge of -3 on the phosphoryl group, whereas the metaphosphate transition state

of the dissociative mechanism has a charge of -1 . These charges are often stabilised by positively charged residues.¹⁴

The active site geometry of riboflavin kinase clearly allows an in-line attack of the 5'-hydroxyl group of FMN on the γ phosphate of ATP (Figure 5). There is no strictly conserved basic residue in the active site of riboflavin kinase (Figure 5). Only Arg36 of flap I represents a rather highly conserved residue which points towards the phosphate-binding site. Other basic residues are not conserved like His32 and Lys39, which are located near the β phosphate and ribose, respectively. In addition, the latter residues are not ideally positioned to interact with the β phosphate as His32 is in a distance of 6.8 Å as measured between P β and N δ . It cannot be ruled out that stabilisation of the transition state involves residues of flap II, which harbours Lys89, Lys91 and Arg93. However, a basic residue is only conserved at position 93 at the end of the loop, which may already have a structural role. These results suggest a direct attack of the 5'-ribityl hydroxyl activated by the general base Glu96 on the metal co-ordinated γ phosphate. Preliminary mutational data (not shown) indicate that the mutation Glu96Gln significantly reduces the enzyme activity. Clearly, further experimental work will be necessary to clarify the role of certain residues during catalysis and to decide which mechanism, associative or dissociative, is used by the enzyme.

Riboflavin kinase: a novel ATP and flavin-binding fold

A structural homology search using the program DALI¹⁵ reveals a number of protein domains that share topological similarity with riboflavin kinase. These include phthalate dioxygenase reductase,¹⁶ flavohemoprotein,¹⁷ flavodoxin reductase¹⁸ and F1-ATPase.¹¹ Superposition of these structures with the riboflavin kinase structure showed that the structural homology only refers to the central β -barrel. In the case of phthalate dioxygenase reductase, flavohemoprotein and flavodoxin, the cofactor-binding site resides in an additional, however unrelated Rossmann-fold type domain and does not coincide with the riboflavin-binding site of riboflavin kinase. Similar β -barrel domains are found in the α and β -subunits of F1-ATPase, which are, however, unrelated to the nucleotide-binding sites at the centre of the oligomer.¹⁹ Therefore, riboflavin kinase does not show any structural relationship to ATP or flavin-binding proteins with known three-dimensional structure.

A characteristic sequence motif of this protein family is associated with the ATP-binding helix H1 that undergoes large rearrangements upon nucleotide binding. The strictly conserved residues Thr45 and Asn47 are preceded by a glycine-rich stretch with a consensus sequence Gly33-x-(Gly)-(Arg, Lys)-Gly-xxxx-Gly-x-ProThrAlaAsn, which contains the invariable motif Gly-x-ProThrAlaAsn.

Due to the deletion of one residue around position 38 in some sequences it is not unambiguous. Only three other residues are strictly conserved: Glu96, Arg121 and Asp139. Whereas Arg121 and Asp139 form a salt bridge that is involved in riboflavin binding, Glu96 probably serves as a general base during phosphoryl transfer or helps to position the ribityl side-chain. However, these residues are not surrounded by characteristic sequence motifs.

The glycine-rich consensus sequence is clearly distinct from motifs associated with other nucleotide-binding proteins as given in the PROSITE database.²⁰ In the P-loop containing structures like F1-ATPase only the hydroxyl group of the threonine residue serves as ligand to the magnesium ion. However, in the latter, it is the end of the P-loop structure between a β -strand and an α -helix preceded by a conserved lysine residue that contacts the β and γ phosphates of ATP.¹¹

Conclusions

Riboflavin kinases represent a ubiquitous protein family with 69 known sequences to date³ that are essential in all organisms as they convert vitamin B2, riboflavin, into the active cofactor FMN. In the present analysis we could elucidate the first structure of this family and demonstrate that it represents a novel fold group in the classification scheme presented by Cheek and co-workers.³ Interestingly, the central β -barrel domain of riboflavin kinase is also observed in a number of other proteins including F1-ATPase, however, with unrelated functions. The structural analysis showed that binding of ATP is an unusually dynamic process and accompanied by large rearrangements of an ATP-binding helix. Other features like the glycine-rich loop (flap I) formed from parts of the ATP-binding helix that covers the triphosphate moiety of ATP are quite typical for kinases. However, this loop is clearly distinct from P-loops or the glycine-rich loop observed in protein kinases. It is likely that a second loop (flap II) that is fixed by lattice contacts in the ADP co-crystals or disordered in the ligand free structure covers the active site during catalysis to exclude water and/or to position the ribityl side-chain of FMN. The divalent metal ion required for enzymatic activity is co-ordinated in an unusual way by both the hydroxyl side-chain oxygen and main-chain carbonyl oxygen of Thr45 in addition to ADP phosphate groups. The proposed reaction mechanism involves an in-line attack of the 5'-hydroxyl group of FMN as a nucleophile on the γ phosphate of ATP. The active site geometry suggests the strictly conserved Asn47 as part of the γ phosphate-binding site and Glu96 as general base as it will be located near the 5' hydroxyl group of the ribityl side-chain of riboflavin that is phosphorylated. However, further biochemical studies will be necessary to verify the proposed role of certain amino acids.

Experimental procedures

Crystallisation

Molecular cloning, overexpression, purification and enzymatic activity measurements of *S. pombe* riboflavin kinase will be described elsewhere. For crystallisation, the protein was dialysed against a buffered solution containing 20 mM Tris-HCl (pH 8.0) and 100 mM NaCl. Crystals were obtained using the sitting-drop vapour-diffusion method by mixing 2 μ l of the protein solution at a concentration of 10 mg/ml and an equal volume of reservoir solution containing 0.1 M Mes-NaOH (pH 6.5), 0.2 M magnesium acetate and 20% (w/v) PEG 8000. The drops were allowed to equilibrate over a reservoir of 0.3 ml of the precipitating buffer. Crystals grew to a maximum dimension of 100 μ m \times 80 μ m \times 50 μ m in about 24 hours at 20 °C. They belonged to space group $P6_122$ with the unit cell constants $a = b = 70.3$ Å, $c = 141.3$ Å and $\alpha = \beta = 90^\circ$, $\gamma = 120^\circ$ with one monomer of 18.9 kDa per asymmetric unit. This results in a Matthews coefficient of 2.6 Å³/Da with a solvent content of about 53%.²¹

Soaking experiments were carried out with riboflavin, FMN, ADP and ATP, respectively, applying concentration between 2 mM and 10 mM. Co-crystallisation experiments with ADP were carried out by mixing wild-type enzyme (10 mg/ml) with 2 mM ADP. Sitting drops were set up from 2 μ l of the complex solution mixed with 2 μ l of 50 mM NaKHPO₄ and 20–22% PEG 8000 at room temperature. Crystals appeared after one week and belonged to space group $P1$ with unit cell constants $a = 38.8$ Å, $b = 45.8$ Å, $c = 51.9$ Å, $\alpha = 90.7^\circ$, $\beta = 111.0^\circ$ and $\gamma = 97.3^\circ$ with two monomers of 18.9 kDa in the asymmetric unit.

Data collection, data processing and phasing

All X-ray data were collected on a MARRResearch345 image plate detector mounted on a Rigaku RU-200 rotating anode operated at 50 mA and 100 kV with λ (Cu K α) = 1.542 Å. Diffraction data used for heavy atom derivative search were collected at 16 °C. Heavy atom derivatives were prepared by soaking the crystals at 20 °C with 2 mM thiomersal (C₉H₉HgNaO₂S), 2 mM 2,6-bischloromercuri-4-nitrophenol, 2 mM tantalum bromide, or with a mixture containing both 2 mM thiomersal and 2 mM 2,6-bischloromercuri-4-nitrophenol for two to three days. For the native crystal, a diffraction limit of 2.9 Å was observed; the diffraction limit for the heavy atom derivatives was between 3.0 Å and 3.8 Å resolution.

Diffraction intensities were integrated and reduced using either the program MOSFLM²² and the CCP4 suite²³ or the HKL suite.²⁴ Initial heavy atom positions for the thiomersal derivative were identified with the program SHELXS²⁵ whereas all others were analysed by the inspection of difference Fourier maps. Heavy atom parameters were refined using MLPHARE.²⁶ Phase calculation was performed between 20 Å and 3.0 Å resolution for the substrate free enzyme. The electron density was improved by solvent flattening using the program DM.²³ Table 1 gives a summary of the data collection and phasing statistics.

All data sets used for refinements were collected under cryogenic conditions at 100 K using an Oxford cryo-stream. For cryo measurements, crystals were transferred into a buffer that contained 30% PEG 400 in

addition to the components of the precipitating buffer. The complex structures were solved by molecular replacement using the program AMORE²⁷ with the structure of the substrate free *S. pombe* riboflavin kinase used as Patterson search model.

Model building and refinement

The 3.0 Å electron density map was of sufficient quality to permit unambiguous chain tracing for about 90% of the model in the first round of model building using the program MAIN.²⁸ Refinement steps carried out consisted of conjugate gradient minimisation, simulated annealing, and B -factor refinement with the program CNS using the mlf target.²⁹ For cross-validation a random test set of 5% of the total number of reflections was excluded from the refinement and used for the calculation of the free R -factor.³⁰ The refinement was carried out on the resulting model until convergence was reached at an R -factor of 22% and an R_{free} of 27% for the substrate free structure. The crystallographic refinement of the ADP complex and the ADP/FMN complex was carried out at 2.0 Å (ADP), 2.45 Å (ADP + FMN) and 1.60 Å (ADP + Zn) employing CNS. After manual rebuilding of the model with MAIN, the final refinement was carried out until convergence was reached.

The Ramachandran plot³¹ calculated with the program PROCHECK³² showed no residues with angular values in forbidden areas: 89.1% (NativII), 89.8% (ADP), 86.7% (ADP + FMN) and 92.2% (ADP + Zn) of the non-glycine residues are in the most favoured regions, 10.9% (NativII), 8.9% (ADP), 13.3% (ADP + FMN) and 7.2% (ADP + Zn) are in additionally allowed regions.

Analysis and graphical representation

Stereochemical parameters were assessed throughout refinement with PROCHECK.³² Secondary structure elements were assigned with STRIDE.³³ Structural Figures were prepared with MOLSCRIPT,³⁴ BOBSCRIPT³⁵ and Swiss-PDB Viewer†.

Atomic co-ordinates

The co-ordinates have been deposited with the Protein Data Bank (accession codes 1N05, 1N06, 1N07 and 1N08) and will be released upon publication.

References

- Schulz, G. (1992). Binding of nucleotides by proteins. *Curr. Opin. Struct. Biol.* **2**, 61–67.
- Vetter, I. R. & Wittinghofer, A. (1999). Nucleoside triphosphate-binding proteins: different scaffolds to achieve phosphoryl transfer. *Q. Rev. Biophys.* **32**, 1–56.
- Cheek, S., Zhang, H. & Grishin, N. V. (2002). Sequence and structure classification of kinases. *J. Mol. Biol.* **320**, 855–881.
- Cooperman, J. M. & Lopez, R. (1984). *Handbook of Vitamins: Nutritional, Biochemical and Clinical Aspects*, Marcel Dekker, New York.
- Mack, M., van Loon, A. P. & Hohmann, H. P. (1998). Regulation of riboflavin biosynthesis in *Bacillus subtilis* is affected by the activity of the flavokinase/

† <http://www.expasy.ch/spdv>

- flavin adenine dinucleotide synthetase encoded by ribC. *J. Bacteriol.* **180**, 950–955.
6. Manstein, D. J. & Pai, E. F. (1986). Purification and characterization of FAD synthetase from *Brevibacterium ammoniagenes*. *J. Biol. Chem.* **261**, 16169–16173.
 7. Nakano, H. & McCormick, D. B. (1990). Rat brain flavokinase: purification, properties, and comparison to the enzyme from liver and small intestine. In *Flavins and Flavoproteins 1990* (Curti, B., Ronchi, S. & Zanetti, E., eds.) pp. 89–92, Walter de Gruyter, Berlin.
 8. Santos, M. A., Jimenez, A. & Revuelta, J. L. (2000). Molecular characterization of FMN1, the structural gene for the monofunctional flavokinase of *Saccharomyces cerevisiae*. *J. Biol. Chem.* **275**, 28618–28624.
 9. Solovieva, I. M., Kreneva, R. A., Leak, D. J. & Perumov, D. A. (1999). The *ribR* gene encodes a monofunctional riboflavin kinase which is involved in regulation of *Bacillus subtilis* riboflavin operon. *Microbiology*, **145**, 67–73.
 10. Merrill, A. H. & McCormick, D. B. (1980). Affinity chromatographic purification and properties of flavokinase (ATP:riboflavin 5'-phosphotransferase) from rat liver. *J. Biol. Chem.* **255**, 1335–1338.
 11. Abrahams, J. P., Leslie, A. G. W., Lutter, R. & Walker, J. E. (1994). Structure at 2.8-Å resolution of F1-ATPase from bovine heart-mitochondria. *Nature*, **370**, 621–628.
 12. Outten, C. E. & O'Halloran, T. V. (2001). Femtomolar sensitivity of metalloregulatory proteins controlling zinc homeostasis. *Science*, **292**, 2488–2492.
 13. Romani, A. M. P. & Maguire, M. E. (2002). Hormonal regulation of Mg²⁺ transport and homeostasis in eukaryotic cells. *BioMetals*, **15**, 271–283.
 14. Matte, A., Tari, L. W. & Delbaere, L. T. J. (1998). How do kinases transfer phosphoryl groups. *Structure*, **6**, 413–419.
 15. Holm, L. & Sander, C. (1993). Protein structure comparison by alignment of distance matrices. *J. Mol. Biol.* **233**, 123–138.
 16. Correll, C. C., Batie, C. J., Ballou, D. P. & Ludwig, M. L. (1992). Phthalate dioxygenase reductase: a modular structure for electron transfer from pyridine nucleotides to [2Fe-2S]. *Science*, **258**, 1604–1610.
 17. Ermler, U., Siddiqui, R. A., Cramm, R. & Friedrich, B. (1995). Crystal structure of the flavohemoglobin from *Alcaligenes eutrophus* at 1.75 Å resolution. *EMBO J.* **14**, 6067–6077.
 18. Ingelmann, M., Bianchi, V. & Eklund, H. (1997). The three-dimensional structure of flavodoxin reductase from *Escherichia coli* at 1.7 Å resolution. *J. Mol. Biol.* **268**, 147–157.
 19. Braig, K., Menz, R. I., Montgomery, M. G., Leslie, A. G. W. & Walker, J. E. (2000). Structure of bovine mitochondrial F1-ATPase inhibited by Mg(2+)ADP and aluminium fluoride. *Struct. Fold. Des.* **8**, 567–573.
 20. Falquet, L., Pagni, M., Bucher, P., Hulo, N., Sigrist, C. J., Hofmann, K. & Bairoch, A. (2002). The PROSITE database, its status in 2002. *Nucl. Acids Res.* **30**, 235.
 21. Matthews, B. W. (1968). Solvent content of protein crystals. *J. Mol. Biol.* **33**, 491–497.
 22. Leslie, A. G. W. (1998). *MOSFLM 6.0 edit.*, Cambridge, UK.
 23. Collaborative Computing Project Number 4 (1994). CCP4 suite: programs for protein crystallography. *Acta Crystallog. sect. D*, **50**, 760–763.
 24. Otwinowski, Z. & Minor, W. (1997). Proceedings of X-ray diffraction data collected in oscillations mode. *Methods Enzymol.* **276**, 307–326.
 25. Sheldrick, G. M., Dauter, Z., Wilson, K. S., Hope, H. & Sieker, L. C. (1993). The application of direct methods of pattern interpretation to high-resolution native protein data. *Acta Crystallogr.* **D49**, 18–23.
 26. Otwinowski, Z. & Minor, W. (1997). Processing of X-ray diffraction data collected in oscillations mode. *Methods Enzymol.* **276**, 307–326.
 27. Navaza, J. (1994). AMoRe: an automated package for molecular replacement. *Acta Crystallog. sect. A*, **50**, 157–163.
 28. Turk, D. (1992). Weiterentwicklung eines Programmes für Molekülgraphik und Elektronendichte-Manipulation und seine Anwendung auf verschiedene Protein-Strukturaufklärungen, PhD Thesis, Technische Universität München, München.
 29. Brünger, A. T. *et al.* (1998). Crystallography & NMR system: a new software suite for macromolecular structure determination. *Acta Crystallog. sect. D*, **54**, 905–921.
 30. Brünger, A. (1992). Free R value: a novel statistical quantity for assessing the accuracy of crystal structures. *Nature*, **355**, 472–475.
 31. Ramachandran, G. N. & Sasisekharan, V. (1968). Conformation of polypeptides and proteins. *Advan. Protein Chem.* **23**, 283–437.
 32. Laskowski, R. A., McArthur, M. W., Moss, D. S. & Thornton, J. M. (1993). PROCHECK—a program to check the stereochemical quality of protein structures. *J. Appl. Crystallog.* **26**, 283–291.
 33. Frishman, D. & Argos, P. (1995). Knowledge-based protein secondary structure assignment. *Proteins: Struct. Funct. Genet.* **23**, 566–579.
 34. Kraulis, P. J. (1991). MOLSCRIPT: a program to produce both detailed and schematic plots of protein structures. *J. Appl. Crystallog.* **24**, 946–950.
 35. Esnouf, R. M. (1997). An extensively modified version of MolScript that includes greatly enhanced coloring capabilities. *J. Mol. Graph. Model.* **15**, 132–134.
 36. Barton, G. J. (1993). ALSCRIPT a tool to format multiple sequences alignments. *Protein Eng.* **6**, 37–40.

Edited by J. Thornton

(Received 14 October 2002; received in revised form 6 January 2003; accepted 6 January 2003)